

Crystalline arrays of submicron-sized particles through colloidal route

B. V. R. Tata^{1,*}, R. G. Joshi¹, D. K. Gupta¹, J. Brijitta and Baldev Raj²

¹Condensed Matter Physics Division, Indira Gandhi Centre for Atomic Research, Kalpakkam 603 102, India

²PSG Institution, Peelamedu, Coimbatore 641 004, India

Advances in colloidal science have made it possible to fabricate crystalline arrays of submicron-sized colloidal particles (popularly known as colloidal crystalline arrays (CCAs) or colloidal crystals (CCs)) with lattice parameters close to the wavelength of light. Light travelling through such crystals experiences a periodic variation of refractive index, analogous to periodic potential energy of an electron in the atomic crystal. This variation in refractive index in three dimensions with hundreds of nanometres periodicity is responsible for photonic band structure in these crystals. Thus these crystals are known as photonic crystals and have several emerging applications such as Bragg diffraction devices, optical filters and switches, sensors, non-bleachable colour materials, etc. Large single crystalline domains are crucial for some of these applications and lithography-based approaches are unrealistic. The present article gives an overview of various self-assembly methods for fabricating polycrystalline as well as large-sized CCAs using suspensions of nearly monodisperse dielectric particles. It also discusses light-based techniques for characterizing their structure and disorder in real and Fourier space. Recent developments in growing CCAs with the desired symmetry and orientation are also highlighted.

Keywords: Colloidal and photonic crystals, confocal microscopy, light scattering, self-assembly.

COLLOIDAL suspensions are ubiquitous and are being used in industrial products such as foods, inks, paints, coatings, cosmetics, photographic films and rheological fluids¹. The multicomponent nature as well as interactions in colloidal systems lead to complex phenomena and hence are of interest in materials science, chemistry and biology. Notable examples include slurries, clays, minerals, aerosols, emulsions and foams; aggregates of surfactant molecules, Au or Ag sols, nanoparticle dispersions of semiconductor quantum dots, silica colloids or polymer latexes in chemistry; and proteins, viruses, bacteria or cells in biology. In many of these colloidal suspensions, the colloidal particles are highly polydisperse in size (i.e. size distribution is broad). The advances that have taken place in synthesizing highly monodis-

perse polymer latex particles and inorganic silica particles in the submicron-size range, paved the way for self-assembling these into colloidal crystalline arrays (CCAs), which are popularly known as colloidal crystals (CCs)¹⁻⁵. Tremendous progress in the synthesis of monodisperse metal nanoparticles (size ≤ 5 nm) capped by thiols has opened up several studies on metal nanoparticle superlattices (also known as metal nanocrystals). Mesoscale organization of metal nanoparticles into crystalline arrays spanning over micrometre range in two and three dimensions as well as at interfaces was achieved. As excellent reviews exist in the literature⁶⁻⁹, the scope of this article is limited to crystalline arrays of monodisperse colloidal dielectric spheres whose diameters are in the submicron range.

Aqueous suspensions of polymethyl-methacrylate (PMMA), polystyrene and silica nanospheres have been studied extensively for their phase behaviour as they can be synthesized in monodisperse form. Sterically stabilized PMMA nanospheres in aqueous medium constitute the best example for hard-sphere suspensions^{2,10}. These particles self-assemble into face-centred-cubic (fcc) (Figure 1a) structure at a volume fraction $\phi \geq 0.5$, whereas charge-stabilized aqueous suspensions of silica and polystyrene nanospheres self-assemble into body-centred-cubic (bcc) (Figure 1b and c) at low volume fractions ($\phi < 0.15$) and into fcc structure at higher volume fractions^{3,4}. The colloidal crystals grown in solvent are

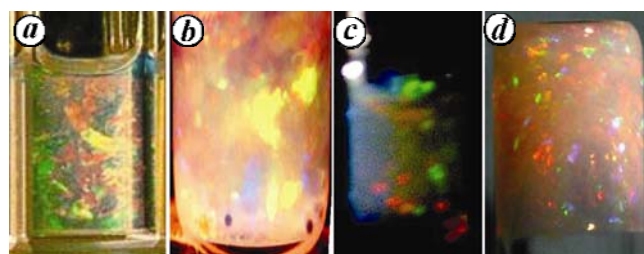


Figure 1. Photographs of photonic crystals or colloidal crystalline arrays (CCAs) exhibiting iridescence under visible light illumination. *a*, Sterically stabilized polymethyl-methacrylate (PMMA) spheres dispersed in decalin-carbon disulphide mixture (adapted from Xia *et al.*¹). *b*, Charge stabilized silica spheres in 90:10 ethylene glycol-water mixture. *c*, Charged polystyrene particles in deionized water. *d*, CCAs of charged polystyrene particles immobilized in a polyacrylamide hydrogel. Sample cell is photographed in an inverted position to show that crystalline order is immobilized and does not flow.

*For correspondence. (e-mail: tata@igcar.gov.in)

extremely fragile, hence are immobilized in a hydrogel medium by growing them first in pre-gel solution and then gelling the solvent by photo-polymerization. The immobilized colloidal crystals in polymer hydrogel medium are shown in Figure 1 *d* and these serve as portable photonic crystals^{11–13}. As the lattice constants of these CCs are in the visible range, they exhibit iridescence due to Bragg diffraction of light and the colours seen in Figure 1 *a–d* are due to iridescence by these crystals. CCAs are periodic dielectric materials, hence many novel properties can be engineered in these materials by controlling their symmetry and lattice constants. The long-range ordering of particles in the structure of CCAs results in a number of unique, potentially useful properties, such as optical diffraction, photonic band gaps, maximal packing density, chemical sensing and high surface/volume ratio^{3,12–17}. Further monodisperse colloidal systems also exhibit gas-like, liquid-like and even glass-like ordering^{3,18}. Hence, they are considered as convenient model systems for fundamental studies of crystallization, melting and glass transition^{3,4,18}.

In charged as well as hard-sphere dispersions, the particle size is fixed and it does not vary with any external stimuli; whereas colloidal dispersions of stimuli-responsive nanogel particles respond to external stimuli such as temperature, pressure and pH by undergoing swelling/deswelling^{19–21}. Aqueous dispersion of poly(*N*-isopropylacrylamide) (PNIPAM) nanogel particles is one such example for stimuli-responsive gel dispersion and the particle size as well as inter-particle interactions^{19–21} vary with temperature, hence they are known as thermo-responsive nanogels. However, it has been reported recently that PNIPAM nanogel particles undergo shrinking when subjected to external pressure²². PNIPAM nanogel particles can be made pH-responsive by incorporating ionizable functional groups (e.g. acrylic acid (AAc)) as co-monomers during the synthesis²³. CCAs prepared by self-assembling PNIPAM nanogel particles in aqueous medium have attracted significant attention due to the ease of tunability of their diffractive properties and the rich phase behaviour²¹.

Here we focus on organizing submicron-sized, nearly monodisperse spherical particles of PMMA, silica, polystyrene and PNIPAM into three-dimensional CCAs in aqueous medium and study their structure, disorder, phase behaviour and diffraction properties using static light scattering (SLS), confocal laser scanning microscopy (CLSM) and UV–visible spectroscopy techniques. Recent methods for growing large single-crystals of CCAs in aqueous medium²⁴ as well as immobilized in polymer hydrogel medium^{25,26} are discussed. Other techniques such as ‘colloidal epitaxy’²⁷ for fabricating large oriented CCAs along the specified crystal directions and ‘holographic optical tweezer’ (HOTA) technique^{28–32} for organizing and manipulating submicron-sized dielectric particles into three-dimensional ordered structures with

desired symmetry and lattice constants are also presented. We have focused on the above-mentioned techniques as these have been extensively used by us in our studies on their structure, dynamics and phase behaviour and in organizing submicron-sized colloidal particles into seed CCAs using HOTA. We also refer to several important results from the literature, citing selective references.

Light-based techniques for characterizing CCAs

Experimental techniques used for characterizing the colloidal dispersions for their particle size, size polydispersity (SPD, defined as standard deviation in particle size/mean diameter), structural ordering and optical properties are briefly discussed. For particle size greater than 300 nm, i.e. the resolution limit of an optical microscope, the 3D real space structure of CCAs can be characterized using a CLSM^{11,33,34}. The CLSM has an improved resolving power compared to a conventional optical microscope. The improved resolution arises due to the use of a confocal pinhole, which causes the photomultiplier tube (PMT) to function as a coherent point detector³⁵. In other words, it sharpens the central peak of the Airy disc with weak outer rings, which gives a small but significant increase in lateral spatial resolution. Further it rejects the light which does not come from the focal plane, thus enabling optical slicing of the sample^{33,34}. Information regarding the stacking of the planes in the crystal in three dimensions is obtained by capturing a series of optical sections (Figure 2 *a*) at various *z*-depths (referred to as *z*-stack) in the sample³³. These *z*-stacks are used for 3D reconstruction of the crystal (Figure 2 *b*). The structural ordering is characterized by image-analysing the *z*-stacks. For obtaining a good statistical average, several *z*-stacks in different regions in the sample are recorded, and quantities such as 2D, 3D pair-correlation functions $g(r)$ and stacking probability α , are determined by performing image analysis on the recorded *z*-stacks³⁴. The (*x*, *y*) particle coordinates are extracted from optical slices using image analysis software such as Leica Qwin and Image J. As each optical slice in a *z*-stack corresponds to a known *z*-distance, the (*x*, *y*, *z*) coordinates for particles in

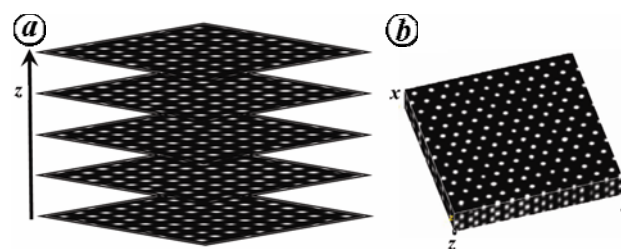


Figure 2. *a*, *z*-Stack of the optical slices showing hexagonal arrangement of 520 nm poly(*N*-isopropylacrylamide) (PNIPAM) particles in each layer. *b*, Three-dimensionally reconstructed image of the five optical slices showing PNIPAM crystalline order.

the z -stack are exactly known and can be used for determining the 3D $g(r)$ which characterizes the real space structure of CCAs in real space³³. The in-plane ordering is characterized by determining 2D $g(r)$, which is calculated using (x, y) particle coordinates in optical slice and averaging over several optical slices. From the first peak position in the 2D $g(r)$, the lattice constant a in the hexagonal closed packed (hcp) plane (Figure 3) can be obtained. For an fcc or hcp structure, the second layer occurs at $\sqrt{2/3} l$, where l is the nearest neighbour distance. Thus by moving the objective lens by a z -distance of $0.82l$, one can track the second layer. For an hcp structure, the lattice constants a and c are related to l by $a = l$ and $c = 2\sqrt{2/3} l$. For fcc structure, $a = \sqrt{2} l$. The stacking sequence and the stacking probability α in a given region of the crystal are determined by merging the consecutive three layers according to the procedure described elsewhere³³.

SLS is the appropriate technique to characterize the structural ordering in less turbid suspensions, where the particle size or the interparticle separation is of the order of the wavelength of light. In SLS, the scattered light intensity $I_s(q)$ from a colloidal dispersion is measured at different scattering wave vectors q , which is related to the scattering angle θ and incident wavelength λ by $q = 4\pi\mu_m \sin(\theta/2)/\lambda$. The time-averaged scattered intensity measured in the vertical-vertical scattering geometry is given as^{3,5}

$$I_s(q) = AP(q)S(q). \quad (1)$$

Here, $S(q)$ is the interparticle structure factor, $P(q)$ the particle structure factor and the constant³ A is due to Rayleigh scattering from N particles of diameter d dispersed in the medium with refractive index μ_m .

$$A = \frac{\pi^4 N d^6}{4\lambda^4} \left[\frac{\mu^2 - 1}{\mu^2 + 2} \right] \frac{I_0}{R^2}. \quad (2)$$

Here, R is the distance between the sample and the detector, and I_0 is the incident intensity. In eq. (2), $\mu = \mu_p/\mu_m$

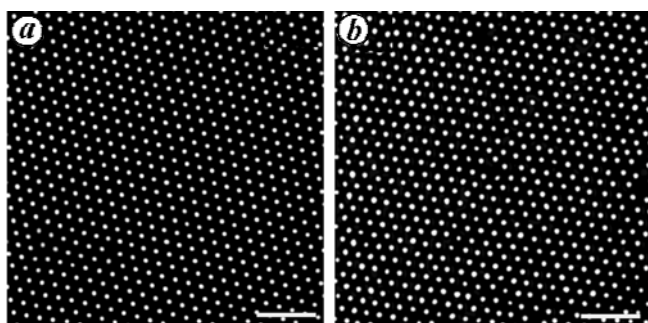


Figure 3. Confocal laser scanning microscope micrographs of (a) 500 nm polystyrene particles and (b) 520 nm PNIPAM microgel particles revealing long-ranged hexagonal arrangement of particles with defects such as point defects and edge dislocations. Scale bar: 5 μm .

is the relative refractive index and μ_p is the particle refractive index. Other scattering techniques for characterizing the crystal structure of strongly turbid CCAs are Kossel analysis and ultra-small-angle X-ray scattering, which are discussed in detail elsewhere⁵.

UV-visible spectroscopy is yet another useful technique to determine the crystal structure of CCAs, provided either the individual colloidal particles or the solvent has no absorption peaks in the UV-visible region¹⁶. The peaks observed either in the extinction (Figure 4) or reflection spectra of CCAs thus correspond to the Bragg reflection from the crystallites that are oriented along the optical path of the beam. The wavelength at which the Bragg reflection occurs can be used for determining the particle number density and the lattice constant^{36,37}. The reflection spectrum³⁸ recorded for CCAs using a UV-visible spectrometer is equivalent to the scattering profile recorded using the SLS technique³. As far as the characterization of the structure of CCAs is concerned, UV-visible spectroscopy and SLS technique are analogous to the energy-dispersive and angle-dispersive X-ray techniques respectively.

In a dynamic light scattering (DLS) experiment, the intensity-intensity autocorrelation function $g^{(2)}(q, t)$ is measured at a given q . The $g^{(2)}(q, t)$ is related to the electric field correlation function $f(q, t)$ by the Siegert relation³ which is given by $g^{(2)}(q, t) = 1 + \beta |f(q, t)|^2$. Particle size and SPD of colloidal particles are determined by measuring $f(q, t)$ in a dilute (non-interacting) dispersion and subjecting $f(q, t)$ to cumulant analysis^{4,33}. In the case of interacting suspensions, $f(q, t)$ is measured at different

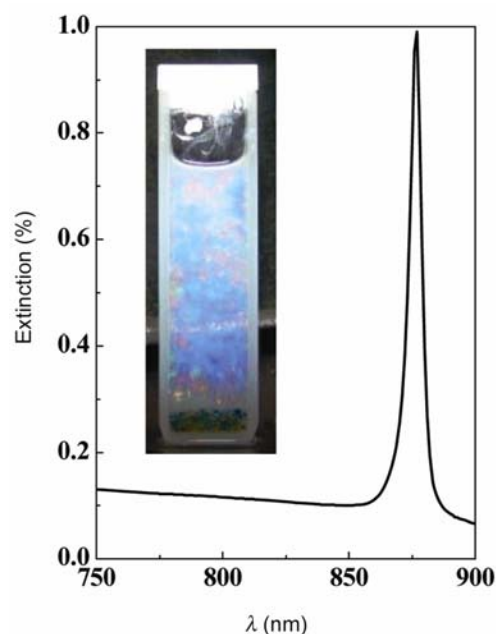


Figure 4. UV-visible spectra of 350 nm PNIPAM nanogel crystals. (Inset) Photograph showing iridescence from PNIPAM nanogel crystals.

q values and analysed for its decay³. It may be mentioned here that particle size and SPD can also be measured from the width of X-ray diffraction (XRD) peaks using Debye–Scherrer formula and imaging techniques such as transmission electron microscopy (TEM), scanning electron microscopy (SEM) and atomic force microscopy (AFM)^{39,40}. However these techniques require samples in dry form and as synthesized suspensions cannot be used for making measurements. Further, these techniques are best suited for opaque nanoparticles prepared using the top-down approach⁴⁰.

Methods for fabricating CCAs

Hard-sphere colloidal crystals

PMMA particles with about 10 nm thick grafted layer of poly(12-hydroxyl stearic acid) dispersed in a mixture of decalin and tetralin (this mixture serves as an index-matching solvent as the refractive index of the solvent closely matches with that of particles)² are known as sterically stabilized suspensions and constitute the best example for hard-sphere suspensions. As hard spheres interact with a potential which is infinite at contact and zero at any separation, the free energy is entirely entropic. For volume fractions above 0.5, entropy favours the ordered crystalline state (fcc) over the disordered liquid state⁴¹. As entropy brings the ordering, hard-sphere colloidal crystals are referred to as entropic crystals⁴². Though fcc is the equilibrium state, random hexagonal closed packed (rhcp) structure is also favoured because the free energy difference between two structures of hard sphere colloidal crystals is very small ($<10^{-3} k_B T$) (ref. 43).

Sedimentation in a gravitational field is a commonly used method for fabricating CCAs by the self-assembly process. Sedimentation provides a simple and efficient method for preparing multilayer assemblies of colloidal particles of size large than 500 nm (ref. 44). This method has a disadvantage with small as well as large particles in growing CCAs, as the former take a long time to sediment or may not sediment at all and the latter deposit too quickly resulting in poor periodicity and tiny crystallites with different orientations. Slow sedimentation of hard-sphere colloidal particles onto a patterned substrate is shown to give large-sized fcc crystals²⁷. Cheng *et al.*⁴¹ have grown large-sized (~ 3 mm) CCAs of hard spheres by developing a method to control the nucleation and growth of hard-sphere crystals that relies on the use of temperature gradients to define a density gradient. In the presence of gravity, the convective flow arising due to temperature gradient provides the mechanism for particle transport and the diffusion regime at the cold end of the temperature gradient provides a zone for controlled nucleation and growth of hard-sphere crystals.

Van Blaaderen *et al.*²⁷ have reported a ‘colloidal epitaxy process’ similar to that employed for epitaxial growth of thin atomic crystalline layers on a template consisting of an oriented single crystal. This is also known as template-directed crystallization. A 500 nm thick fluorescent polymer layer with holes made using electron beam lithography has been used as a template. The thickness is close to the particle radius (525 nm) of the fluorescent silica spheres. Controlled layer-by-layer growth was achieved by slow sedimentation of the particles onto the substrate. By preparing a pattern of holes matching with the (100) plane of the fcc crystal, a pure crystal of several millimetres thickness was formed. CLSM has been used to characterize the structure and stacking of the crystal structure. The single crystal grown on the (100) plane is found to be fcc. The structures grown on the (110) plane are found to be less dense and have no twinning directions. It is shown that creating an intentional lattice mismatch helps in the growth of different defect structures. The manipulative capabilities of colloidal epitaxy are also demonstrated by making simple changes in the lattice spacing between two adjacent (100) planes. Hoogenboom *et al.*⁴⁵ have demonstrated that it is possible to grow metastable hard-sphere crystals with hcp structure by colloidal epitaxy. They found that the stacking sequence could be dictated by the template, thus allowing the growth any of the intermediate ‘random’ stacking sequences.

Charged colloidal crystals

Monodisperse charge-stabilized colloidal particles (e.g. polystyrene and silica) in aqueous medium undergo electrostatic interactions and exhibit different structural orders depending on the range and strength of the interactions. The interparticle interaction $U(r)$ between charged colloidal particles is predominantly screened Coulomb repulsive and is given by

$$U(r) = \frac{Z^2 e^2}{\epsilon} \left[\frac{e^{\kappa a}}{1 + \kappa a} \right]^2 \frac{e^{-\kappa r}}{r}, \quad (3)$$

where a is the radius of the particle, Ze the effective charge and is related to surface charge density $\sigma = Ze/\pi d^2$, ϵ the dielectric constant of the medium and κ is the inverse Debye screening length defined as

$$\kappa^2 = \frac{4\pi e^2}{\epsilon k_B T} (n_p Z + C_s). \quad (4)$$

$U(r)$ can be tailored by varying suspension parameters such as particle concentration n_p , surface charge density on the particle σ and salt concentration C_s . At moderate

charge density and for very low values of C_s , charge-stabilized suspensions self-assemble into either a bcc or fcc structure depending on the volume fraction. Experimental phase diagrams showing stable bcc, fcc and liquid-like phases of charged colloids have been reported^{3,4}. Stable CCAs of charged polystyrene spheres in aqueous medium can be fabricated by preparing a suspension with volume fraction above 0.005 and deionizing (removing the salt ions in the solvent) the suspensions using a mixed bed of ion-exchange resins²⁵. Deionized silica suspensions can be self-assembled into a crystalline state by introducing small amounts of sodium hydroxide or pyridine, which helps in increasing the surface charge due to enhanced dissociation of weakly acidic silanol groups²⁶. When the surface charge density on the particles is high, the suspensions undergo phase separation in the form of gas–solid transition⁴⁶ with solid regions being crystalline or glass-like, hence are not useful for fabricating CCAs. Tata *et al.*^{3,47} have reported millimetre-sized CCAs of silica particles (Figure 1 *b*) by redispersing them in a 90 : 10 ethylene glycol : water mixture. The enhanced viscosity of the solvent slows down the diffusion of the particles and helps in growing large size crystals. Further the 90 : 10 ethylene glycol : water mixture helped in suppressing multiple scattering of light due to close index matching with particles and in providing evidence for the existence of propagating long-wavelength transverse modes^{3,47} in colloidal crystals.

It is possible to grow sub-millimetre to millimetre-sized charged colloidal crystals^{2,3,24–27} in a solvent under laboratory environment. Recently, there have been reports by Japanese groups of growing large size charged colloidal single crystals in water as well as in a polymer hydrogel medium^{12,25}. Sawada *et al.*²⁴ have developed a simple method to grow centimetre-sized single crystal domains of polystyrene and silica particles suspended in deionized water. The method employs high shear rates on a colloidal suspension, which can freeze into an equilibrium crystal structure under zero shear and create a nonequilibrium ordered structure. The shear-induced ordering is governed by the direction of the streamline flow and the shear gradient. If the nonequilibrium ordered structure at high shear rates is close to the equilibrium structure at rest, an abrupt release of the high shear rate (i.e. shear quenching) would result in a large size single crystal. Figure 5 *a* shows the schematic of the experimental set-up and Figure 5 *b* shows the large size (~8 cm) CCAs of charged colloids grown by application of controlled shear. To avoid degradation of the crystalline quality and make them portable, these large-size single crystals are immobilized using photo-polymerization technique²⁵.

Fabrication of large-size CCAs by shear quenching of colloidal suspensions in thin, flat capillaries²⁴, though simple and adoptable to suspensions of various kinds of submicron-sized particles, the crystals grown are large in

size in two dimensions and limited to less than a millimetre in thickness. This limitation has been circumvented by Murai *et al.*²⁶ using a one-dimensional growth technique based on pH gradient which is analogous to Bridgeman temperature gradient method adopted for growing atomic/molecular crystals. This method is illustrated schematically in Figure 6 *a*. Murai *et al.*²⁶ have used pyridine (Py) gradient to grow CCAs of silica particles. The surface charge on silica particles is enhanced using NaOH by adjusting the pH of the dispersion to 4.5. Since Py is a weak base ($pK_a = 5.42$), its diffusion in undissociated form in the suspension helps in fine-tuning the surface charge, and hence the growth of CCs. Silica particle suspension with $pH = 4.5$ was introduced into a PMMA cell with a polyacrylamide-based gel membrane at its bottom and the cell was kept in contact with the Py reservoir. Suspension pH was maintained acidic throughout the experiment. Py from its reservoir diffuses slowly through the gel membrane into the suspension. Diffusion of Py results in a concentration gradient along the height of the suspension. In the high-Py concentration region, silica particles gain more charge due to dissociation of silanol groups and get into an ordered state, whereas the region with low Py concentration remains disordered. Thus the rate of growth of the crystal is controlled by controlling the rate of diffusion of Py into the suspension. The large-size CCA of silica particles grown using this method is shown in Figure 6 *b* (ref. 26).

SLS technique has been extensively used to characterize the structural ordering in aqueous suspension of polystyrene and silica colloids^{3,46,47}. If the sample (usually a cylindrical-shaped glass or quartz cuvette containing the suspension) exhibits iridescence (Figure 1) for visible light, it is a clear signature that particles have assembled into a crystalline array and the iridescence arises due to

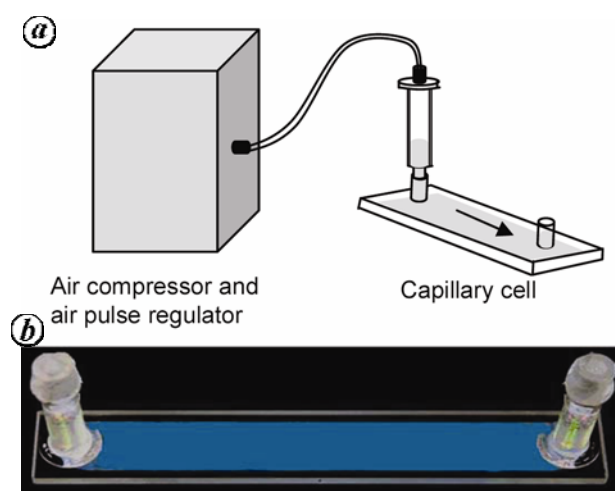


Figure 5. *a*, Schematic of the experimental set-up used to grow large-sized uniform colloidal crystals through shear-induced crystallization. *b*, Photograph of the large-sized colloidal single crystal grown by shear-induced crystallization (adapted from Sawada *et al.*²⁴).

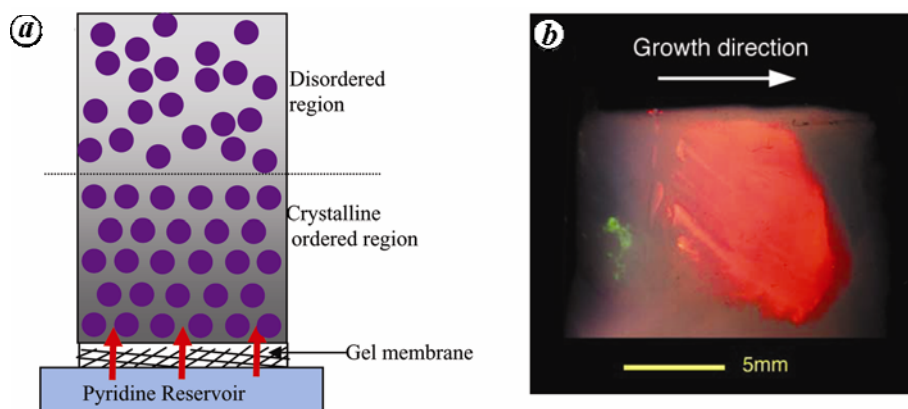


Figure 6. *a*, Schematic of the experimental set-up used to grow one-directional colloidal crystal driven by diffusion of a weak base. *b*, Photograph of the large-sized colloidal single crystal of charged silica particles grown by slow diffusion of pyridine (photograph: courtesy from Yamanaka²⁶).

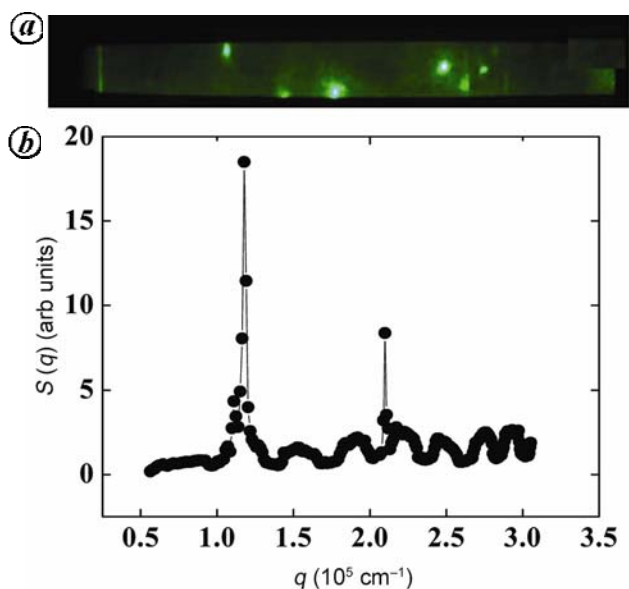


Figure 7. *a*, Photograph of the Bragg spots captured for charged colloidal crystals. *b*, Structure factor $S(q)$ versus scattering wave vector q shows sharp peaks corresponding to a bcc ordering in colloidal crystals.

Bragg diffraction of light by the crystallites. If one observes Bragg spots (Figure 7*a*) under laser light illumination, it implies that the sample contains several large-sized crystallites. The Bragg spots are captured using a detector (photomultiplier tube) mounted on a goniometer which is similar to an XRD pattern of atomic crystals^{18,46}. The laser diffraction pattern (Figure 7*b*) thus recorded is analysed for characterizing the structure of CCAs in the sample cell. Small-angle X-ray scattering⁴ (SAXS) and ultra-small-angle X-ray scattering⁵ (USAXS) techniques have also been employed to study the structural ordering in dense and highly turbid suspensions. As mentioned earlier, UV-visible spectroscopy is another technique that has been extensively used for characterizing the structure and optical properties of CCAs^{36–38}. The

Bragg peaks in reflection or transmission spectra are analysed for determining the lattice constants of CCAs³⁶ and also for characterizing the structure³⁸.

Colloidal crystals of stimuli-responsive gel particles

Aqueous suspensions of stimuli-responsive PNIPAM and PNIPAM-*co*-acrylic acid (PNIPAM-*co*-AAc) particles can be synthesized in different sizes by free-radical polymerization²⁰. PNIPAM nanoparticles are thermo-responsive (size decreases gradually below volume phase transition (VPT) $\sim 34^\circ\text{C}$) and undergo sudden collapse in volume at VPT²⁰, whereas PNIPAM-*co*-AAc particles are not only responsive to temperature but also to pH²³. Purified suspensions of monodisperse PNIPAM and PNIPAM-*co*-AAc nanogel particles can be self-assembled into ordered structures beyond certain particle concentration. Purified suspensions can be concentrated by centrifugation, evaporation or by ultra-filtration techniques. The concentrated suspensions of nanogel particles are in a glass-like disordered state due to kinetic arrest of the particles and can be transformed to CCAs by repeatedly annealing above VPT²⁰. Heating also improves the quality of the crystalline order by annealing out the defects. Tang *et al.*⁴⁸ have prepared PNIPAM-*co*-AAc microgel crystals by evaporating the solvent in PNIPAM suspension at a temperature higher than 34°C and then allowing the concentrated suspension to reach an equilibrium state at 19°C for 1 week. They observed the gradual growth of the crystallites at pH 4.4 and at 19°C . Joshi *et al.*³⁶ have observed crystalline order upon heating the concentrated suspensions obtained by ultrafiltration technique. Use of ultrafiltration technique is advantageous as it not only purifies the suspension but also aids in concentrating it.

Brijitta *et al.*^{20,33} have prepared crystalline arrays of 273 and 520 nm PNIPAM nanogel particles and studied

their structure, disorder and melting using SLS and CLSM techniques²¹. The iridescence from CCAs of 273 nm nanogel particles with particle concentration $n_p = 8.71 \times 10^{13} \text{ cm}^{-3}$ is shown in Figure 8a (inset). The Bragg spots show very high intensity and the Bragg peak (Figure 8a) is found to be sharp, suggesting that the sample consists of good-quality single crystalline domains. The stability of these crystallites against temperature was studied by monitoring the Bragg peak intensity, $I_{\max}(q)$ as a function of temperature (Figure 8b)^{20,21}. The sudden decrease in the Bragg peak intensity at $T = 24^\circ\text{C}$ is due to melting of crystals into a liquid-like order (Figure 8c). Alsayed *et al.*⁴⁹ have also studied the melting of PNIPAM microgel crystals using digital video microscopy and found that pre-melting occurs at grain boundaries and dislocations located within the crystals.

As mentioned earlier, CLSM is a useful technique to study the crystal structure and disorder in real space. Brjitta *et al.*³³ have used CLSM to study the structure as well as stacking disorder in CCAs of PNIPAM particles of 520 nm diameter. Two crystalline samples have been prepared using two different routes: (i) as-prepared sample: by solidifying the shear melted colloidal liquid and (ii) re-crystallized sample: slow cooling of the colloidal liquid. Analysis of stacking sequence of layers recorded on the as-prepared sample revealed the existence of stacking disorder with an average stacking probability $\alpha = 0.42$. This value of α together with the analysis of three-dimensional pair-correlation function $g(r)$, revealed the structure of nanogel crystals in the as-prepared sample to be random hexagonal close packing³³. The as-prepared sample when heated from 25°C to 40°C melted into an isotropic colloidal liquid, which upon cooling

back to 25°C with a cooling rate of $0.15^\circ\text{C}/\text{min}$ was found to recrystallize into a fcc structure³³. CLSM studies on PNIPAM microgel crystals have revealed that unlike in hard sphere or charged colloidal crystals, the crystal structure of soft PNIPAM spheres depends on the method by which these are re-crystallized. Further, shear and temperature play an important role in controlling the structure and disorder in these crystals.

Colloidal crystals of non-spherical and Janus particles

In colloidal science, a sphere represents the simplest shape and colloidal particles of sub-micron size could easily be developed by the minimization of interfacial free energy¹. There are only a few methods available for synthesizing well-defined sizes and shapes. One approach that was followed for preparing polystyrene and PMMA ellipsoids is synthesizing monodisperse spherical particles followed by dispersing them in an elastic matrix and then transforming them into uniform ellipsoids by stretching the matrix at a temperature higher than the glass transition temperature of the polymer latexes⁵⁰. The ellipsoidal colloidal particles are collected as a stable dispersion in a solvent by removing the matrix materials by chemical methods. The polystyrene ellipsoids are self-assembled into 3D crystalline lattice having both positional and orientational ordering first by creating surface charges on the particles through functionalization and then allowing them to undergo positional ordering into a 3D lattice through repulsive electrostatic interparticle interactions similar to those of charged polystyrene colloids described above. The orientational ordering is achieved subsequently by applying an external electric field⁵⁰. In the case of magnetically active non-spherical particles (e.g. ferrofluids), orientational ordering is achieved with the application of magnetic field. Rossi *et al.*⁵¹ have synthesized cubical, hollow silica particles and self-assembled them into cubic colloidal crystals in aqueous medium by controlling the anisotropic depletion interaction between cubes through the addition of non-adsorbing polymer chains or submicron-sized PNIPAM gel particles as depletion agents. Alternating electric field was found to assist crystallization as well as in improving the uniformity of the cubic pattern. There are limited reports to achieve targeted ordered self-assembled structures through the designed building blocks such as patchy particles⁵² or Janus particles⁵³ (spherical particles with two patches). The experimental work by Chen *et al.*⁵³ in investigating the self-assembly into 2D kagome lattice (an arrangement of intertwined triangles) has shown that control on the structure can be gained using only two circular patches (i.e. by Janus particles) and by properly tailoring the patch width. Romano and Scotino⁵² have reported self-assembly of 3D crystals of Janus particles

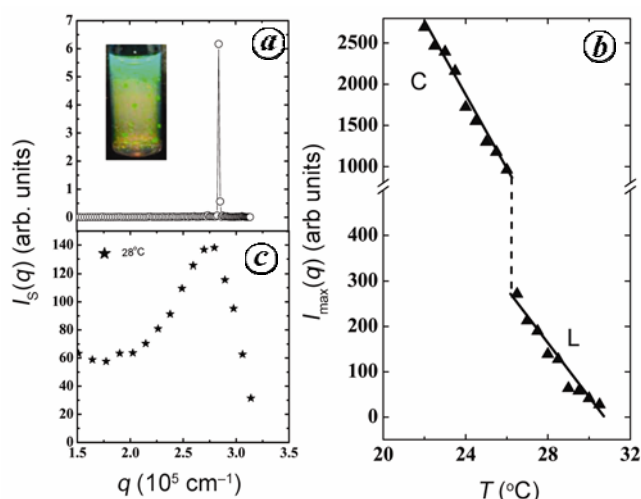


Figure 8. *a*, $I_s(q)$ as a function of q for sample at $T = 23^\circ\text{C}$. (Inset) Photograph of the PNIPAM microgel suspension exhibiting iridescence under visible light illumination. *b*, Bragg peak intensity $I_{\max}(q)$ as a function of T . C and L represent the temperature regions where sample exhibited crystalline (C) and liquid-like (L) behaviour respectively. *c*, $I_s(q)$ as a function of q for sample at $T = 28^\circ\text{C}$ exhibiting liquid-like order.

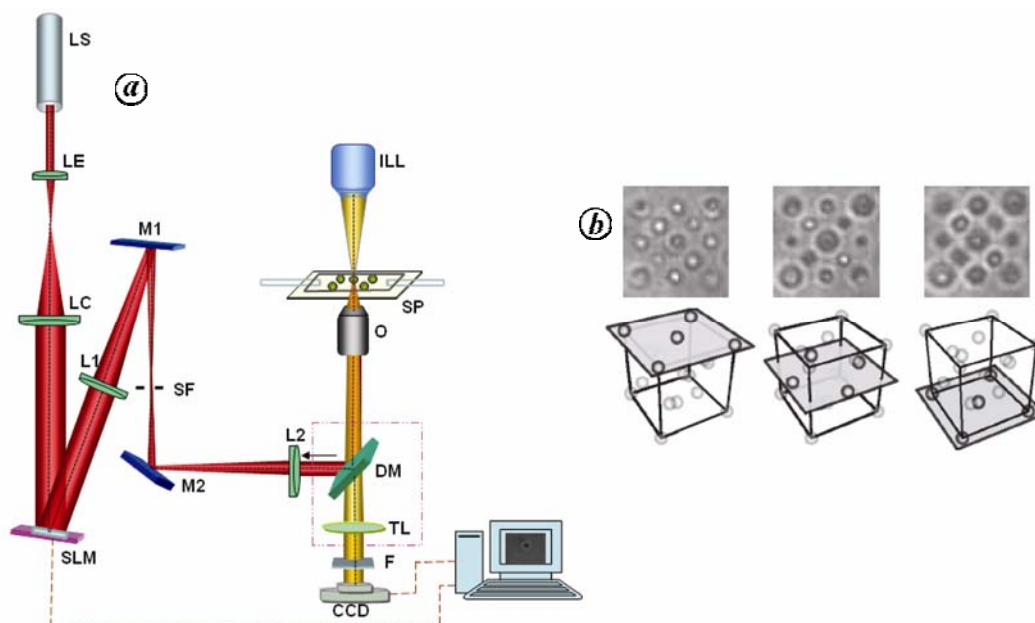


Figure 9. *a*, Schematic diagram of a holographic optical tweezer set-up. (LS, TEM₀₀ Laser source; LE, LC, Beam expander lenses; SLM, Spatial light modulator; L1, L2, Telescopic lenses; M1, M2, Mirrors; SF, Spatial filter; DM, Dichroic mirror; O, Microscope objective; SP, Sample plane; ILL, Illumination source; TL, Tube lens; F, Filter; CCD, Charge couple device). *b*, Optically trapped diamond unit cell constructed from 18 silica spheres of 2 μm diameter suspended in water (adapted from Benito *et al.*³²).

with mixed morphologies (i.e. coexisting regions of fcc and hcp structures) similar to hard-sphere colloids. Thus non-spherical colloidal particles self-assemble into CCAs with non-cubic closed packed structures under suitable conditions. These crystalline arrays offer the possibility of tuning the photonic band-gap properties (i.e. closing and opening the gap) by controlling the orientation of the non-spherical particles using external fields or by controlling the number of patches and width of the patches in the case of patchy colloids.

Assembling colloidal particles using holographic optical tweezer arrays

The methods discussed for fabricating CCAs using colloidal suspension are based on the self-assembly process and assembled structures are restricted to bcc, fcc and rhcp structures. The lattice constants of these structures are determined by particle concentration. Here we discuss another method based on the HOTA technique that offers the advantage of designing and fabricating CCAs with the desired symmetry and lattice constants.

The HOTA technique²⁸ uses a computer-generated hologram to produce multiple focused laser beams (i.e. multiple traps) from a single laser beam which can be translated in real time in three dimensions^{28–31}. Using multiple traps, it is possible to use HOTA as a micro or nanoassembler^{29–31}. We have designed an optical layout which is shown schematically in Figure 9*a* for assembling a HOTA set-up. The set-up consists of a continuous-wave

TEM₀₀ laser beam which is expanded and then collimated by the lenses LE and LC. The collimated beam is made to be incident on the spatial light modulator (SLM) which modulates the phase of the light and the resulting beams are focused into an array of optical traps through a telescopic arrangement (formed by lenses L1 and L2) and a high numerical aperture objective (O) of a commercial inverted microscope. The required trap patterns with desired symmetry and lattice constants are generated using new or existing algorithms³⁰. The trap pattern can be changed dynamically by using a computer to continually refresh the mask on SLM. Sample cells containing suspension of colloidal particles are placed in the sample plane (SP) which is illuminated using a light source and imaged using CCD camera.

The assembly through HOTA involves trapping of particles and perfectly positioning them at the desired locations according to the trapping pattern and then immobilization of particles in pre-gel solution by chemical or photo-polymerization. HOTA has been used to create 1D and 2D arrays of trapped particles using methods which are reviewed in detail elsewhere⁵⁴. Formation of 3D structures of silica particles in a gelatin gelling medium has been demonstrated by Jordan *et al.*²⁹. These structures remain intact even if the laser beam is removed after setting up in a gelatin gel matrix. Leach *et al.*³⁰ have developed two types of algorithms for generating 3D structures. One algorithm is interactive and can be used for designing symmetric structures such as cubic, while the other algorithm is too slow for interactive use but

allows designing arbitrary structures such as diamond unit cell (Figure 9b). Using these algorithms, they³⁰ have fabricated cubic and diamond structures of silica particles over length scales of several tens of microns. Benito *et al.*³² have developed a direct assembly method, where HOTA is used for trapping the particles and colloidal interactions are adjusted for adhesion of trapped particles. The adhesion of trapped particles was achieved by adjusting the polymer concentration in the suspension. The presence of polymer chains in between the particles results in depletion interaction which is attractive in nature and helps in the adhesion of particles trapped by HOTA.

Using directed assembly, Benito *et al.*³² have created a simple cubic structure of polystyrene spheres. For spherical particles, the lowest energy structure is always one of the closed-packed arrangements (fcc or hcp). The simple cubic structure is difficult to realize by self-assembly, but is straightforward using directed assembly method. Uses of HOTA in organizing 3D structure of *Escherichia coli*⁵⁵ as well as colloidal structure with DNA as connectors have also been demonstrated⁵⁶. Thus HOTA provides the possibility of assembling colloidal particles into small seed colloidal crystals with the desired symmetry, lattice constants and tunable defects, which can be used for fabricating templates for photonic band-gap materials³².

Conclusion

We have presented a number of methods based on self-assembly for growing large-size crystalline arrays through the colloidal route. The methods discussed are applicable for a wide size range (nm to μm) as well as for a variety of submicron-sized particles (PMMA, polystyrene, silica, PNIPAM, etc.). CCAs grown in a solvent can be immobilized in polymer hydrogels and serve as photonic crystal materials. These photonic crystals diffract UV, visible and near-infrared light depending on the lattice spacing. The diffraction phenomena resemble those of opals, which are closed-packed arrays of monodisperse silica spheres. Self-assembly is usually restricted to the construction of close-packed structure with spherical particles. However, non-spherical colloidal particles and patchy particles provide complexity and non-cubic closed packed structures with new types of functionality. Seed crystals of non-close packed structures with desired symmetry and lattice constants can be fabricated using techniques such as HOTA. It is also possible to fabricate CCAs embedded with artificial defects for the purpose of using these as waveguides, light emitters, etc. We have also discussed, in brief, techniques for characterizing the crystal structure, disorder and stability in real and Fourier spaces.

1. Xia, Y., Gates, B., Yin, Y. and Lu, Y., Monodispersed colloidal spheres: old materials with new applications. *Adv. Mater.*, 2000, **12**, 693–713.

2. Pusey, P. N. and Van Meegen, W., Phase behaviour of concentrated suspensions of nearly hard colloidal spheres. *Nature*, 1986, **320**, 340–342.
3. Tata, B. V. R. and Jena, S. S., Ordering, dynamics and phase transitions in charged colloids. *Solid State Commun.*, 2006, **139**, 562–580.
4. Chakraborti, J., Krishnamurthy, H. R., Sengupta, S. and Sood, A. K., Density functional theory of freezing of charged-stabilized colloidal suspensions. In *Ordering Phase Transitions in Charged Colloids* (eds Arora, A. K. and Tata, B. V. R.), VCH Publishers, New York, 1996, pp. 235–257.
5. Arora, A. K. and Tata, B. V. R., Interactions, structural ordering and phase transitions in colloidal dispersions. *Adv. Colloids Interface Sci.*, 1998, **78**, 49–97.
6. Rao, C. N. R., Kulkarni, G. U. and John Thomas, P., Metal nanoparticles and their assemblies. *Chem. Soc. Rev.*, 2000, **29**, 27–35.
7. Kulkarni, G. U., John Thomas, P. and Rao, C. N. R., Mesoscale organization of metal nanocrystals. *Pure Appl. Chem.*, 2002, **74**, 1581–1591.
8. Kimura, K. and Pradeep, T., Functional noble metal nanoparticle superlattices grown at interfaces. *Phys. Chem. Chem. Phys.*, 2011, **13**, 19214–19225.
9. Sidhaye, D. S. and Prasad, B. L. V., Many manifestations of digestive ripening: monodispersity, superlattices and nanomachining. *New J. Chem.*, 2011, **35**, 755–763.
10. van Meegen, W. and Underwood, S. M., Glass transition in colloidal hard spheres: mode-coupling theory analysis. *Phys. Rev. Lett.*, 1993, **70**, 2766–2769.
11. Joannopoulos, J. D., Pierre, R., Villeneuve and Fan, S., Photonic crystals: putting a new twist on light. *Nature*, 1997, **386**, 143–149.
12. Iwayama, Y., Yamanaka, J. and Takiguchi, Y., Optically tunable gelled photonic crystal covering almost the entire visible light wavelength region. *Langmuir*, 2003, **19**, 977–980.
13. Norris, D. J. and Vlasov, Y. A., Chemical approaches to three-dimensional semiconductor photonic crystals. *Adv. Mater.*, 2001, **13**, 371–376.
14. Wijnhoven, J. E. G. J. and Vos, W. L., Preparation of photonic crystals made of air spheres in titania. *Science*, 1998, **281**, 802–804.
15. Pan, G., Kesavamoorthy, R. and Asher, S. A., Optically nonlinear Bragg diffracting nanosecond optical switches. *Phys. Rev. Lett.*, 1997, **78**, 3860–3863.
16. Holtz, J. H. and Asher, S. A., Polymerized colloidal crystal hydrogel films as intelligent chemical sensing materials. *Nature*, 1997, **389**, 829–832.
17. Tarhan, I. I., Watson and George, H., Photonic band structure of fcc colloidal crystals. *Phys. Rev. Lett.*, 1996, **76**, 315–318.
18. Tata, B. V. R., Colloidal dispersions and phase transitions in charged colloids. *Curr. Sci.*, 2001, **80**, 948–958.
19. Pelton, R., Temperature-sensitive aqueous microgels. *Adv. Colloid Interface Sci.*, 2000, **85**, 1–33.
20. Brijitta, J., Tata, B. V. R. and Kaliyappan, T., Phase behaviour of poly(*N*-isopropylacrylamide) nanogel dispersions: temperature dependent particle size and interactions. *J. Nanosci. Nanotechnol.*, 2009, **9**, 5323–5328.
21. Tata, B. V. R., Brijitta, J. and Joshi, R. G., Thermo-responsive nanogel dispersions: dynamics and phase behaviour. *Int. J. Adv. Eng. Sci. Appl. Math.*, 2011; doi: 10.1007/s12572-010-0016-5.
22. Liotor-Santos, J. J., Sierra-Martin, B., Vavrin, R., Hu, Z., Gasser, U. and Fernandez-Nieves, A., Deswelling microgel particles using hydrostatic pressure. *Macromolecules*, 2009, **42**, 6225–6230.
23. Snowden, M. J., Chowdhry, B. Z., Vincent, B. and Morris, G. E., Colloidal copolymer microgels of *N*-isopropyl acrylamide and acrylic acid: pH ionic strength and temperature effects. *J. Chem. Soc., Faraday Trans.*, 1996, **92**, 5013–5016.
24. Sawada, T., Suzuki, Y., Toyotama, A. and Iyi, N., Quick fabrication of gigantic single-crystalline colloidal crystals for photonic

- crystal applications. *Jpn. J. Appl. Phys.*, 2001, **40**, L1226–L1228.
25. Kanai, T., Sawada, T. and Yamanaka, J., Fabrication of large-area silica colloidal crystals immobilized in hydrogel film. *J. Ceram. Soc. Jpn.*, 2010, **118**, 370–373.
26. Murai, M. *et al.*, Unidirectional crystallization of charged colloidal silica due to the diffusion of a base. *Langmuir*, 2007, **23**, 7510–7517.
27. Van Blaaderen, A., Ruel, R. and Wiltzius, P., Template-directed colloidal crystallization. *Nature*, 1997, **385**, 321–324.
28. Curtis, J. E., Koss, B. A. and Grier, D. G., Dynamic holographic optical tweezers. *Opt. Commun.*, 2002, **207**, 169–175.
29. Jordan, P., Clare, H., Flendrig, L., Leach, J., Cooper, J. and Padgett, M., Permanent 3D microstructures in a polymeric host created using holographic optical tweezers. *J. Mod. Opt.*, 2004, **51**, 627–632.
30. Leach, J., Sinclair, G., Jordan, P., Courtial, J., Padgett, M. J., Cooper, J. and Laczik, Z. J., 3D manipulation of particles into crystal structures using holographic optical tweezers. *Opt. Express*, 2004, **12**, 220–226.
31. Sinclair, G., Jordan, P., Courtial, J., Padgett, M., Cooper, J. and Laczik, Z. J., Assembly of 3-dimensional structures using programmable holographic optical tweezers. *Opt. Express*, 2004, **12**, 5475–5480.
32. Benito, D. C. *et al.*, Constructing 3D crystal templates for photonic band gap materials using holographic optical tweezers. *Opt. Express*, 2008, **16**, 13005–13015.
33. Brijitta, J., Tata, B. V. R., Joshi, R. G. and Kaliyappan, T., Random hcp and fcc structures in thermoresponsive microgel crystals. *J. Chem. Phys.*, 2009, **131**, 074904–074911.
34. Tata, B. V. R. and Raj, B., Characterization of soft condensed matter using confocal microscopy. In *Advances in Materials Characterization* (eds Raj, B., Amarendra, G. and Manghnani, M. H.), University Press, Hyderabad, 2006, pp. 123–156.
35. Sheppard, C. J. R. and Shotton, D. M., *Confocal Laser Scanning Microscopy*, BIOS Scientific Publishers, Oxford, UK, 1997.
36. Joshi, R. G., Tata, B. V. R. and Brijitta, J., Pressure tuning of Bragg diffraction in stimuli responsive microgel crystals. *AIP Conf. Proc.*, 2010, **1349**, 208–209.
37. Weissman, J. M., Sunkara, H. B., Tse, A. S. and Asher, S. A., Thermally switchable periodicities and diffraction from mesoscopically ordered materials. *Science*, 1996, **274**, 959–963.
38. Zhou, H., Xu, S., Sun, Z., Du, X. and Xie, J., Rapid determination of colloidal crystal's structure by reflection spectrum. *Colloids Surf. A – Physicochem. Eng. Aspects*, 2011, **375**, 50–54.
39. Pradeep, T., *Nano: The Essentials, Understanding Nanoscience and Nanotechnology*, Tata McGraw-Hill, New Delhi, 2007.
40. Raychaudhuri, A. K., Nanolithography and nanomanipulation. In *The Chemistry of Nanomaterials: Synthesis, Properties and Applications* (eds Rao, C. N. R., Muller, A. and Cheetham, A. K.), Wiley-VCH Verlag GmbH & Co. KGaA, Weinheim, 2004, pp. 688–723.
41. Cheng, Z., Russel, W. B. and Chaikin, P. M., Controlled growth of hard-sphere colloidal crystals. *Nature*, 1999, **401**, 893–895.
42. Cheng, Z., Zhu, J., Russel, W. B. and Chaikin, P. M., Phonons in entropic crystal. *Phys. Rev. Lett.*, 2000, **85**, 1460–1463.
43. Frenkel, D. A. and Ladd, A. J. C., New Monte-Carlo method to compute the free-energy of arbitrary solids. Application to the fcc and hcp phases of hard spheres. *J. Chem. Phys.*, 1984, **81**, 3188–3193.
44. Nakamura, H., Colloidal crystals – self-assembly of monodispersed colloidal particles. *R&D Review of Toyota CRDL*, 2004, **39**, 33–39.
45. Hoogenboom, J. P., Yethiraj, A., van Langen-Suurling, A. K., Romijn, J. and van Blaaderen, A., Epitaxial crystal growth of charged colloids. *Phys. Rev. Lett.*, 2002, **89**, 256104(1)–256104(4).
46. Mohanty, P. S., Tata, B. V. R., Toyotama, A. and Sawada, T., Gas–solid coexistence in highly charged colloidal suspensions. *Langmuir*, 2005, **21**, 11678–11683.
47. Tata, B. V. R., Mohanty, P. S., Valsakumar, M. C. and Yamanaka, J., Long-wavelength transverse modes in charged colloidal crystals. *Phys. Rev. Lett.*, 2004, **93**, 268303–268306.
48. Tang, S., Hu, Z., Zhou, B., Cheng, Z., Wu, J. and Marquez, M., Melting kinetics of thermally responsive microgel crystals. *Macromolecules*, 2007, **40**, 9544–9548.
49. Alsayed, A. M., Islam, M. F., Zhang, J., Collings, P. J. and Yodh, A. G., Premelting at defects within bulk colloidal crystals. *Science*, 2005, **309**, 1207–1210.
50. Lu, Y., Yin, Y. and Xia, Y., Three-dimensional photonic crystals with non-spherical colloids as building blocks. *Adv. Mater.*, 2001, **13**, 415–420.
51. Rossi, L., Sacanna, S., Irvine William, T. M., Chaikin Paul, M., Pineb David, J. and Philipse Albert, P., Cubic crystals from cubic colloids. *Soft Matter*, 2011, **7**, 4139–4142.
52. Romano, F. and Sciortino, F., Patchy from the bottom up. *Nature Mater.*, 2011, **10**, 171–173.
53. Chen, Q., Chul Bae, S. and Granick, S., Directed self-assembly of a colloidal kagome lattice. *Nature*, 2011, **469**, 381–384.
54. Grier, D. G., A revolution in optical manipulation. *Nature*, 2003, **424**, 810–816.
55. Jordan, P. *et al.*, Creating permanent 3D arrangements of isolated cells using holographic optical tweezers. *Lab Chip*, 2005, **5**, 1224–1228.
56. Castelino, K., Satyanarayana, S. and Sittiet, M., Manufacturing two- and three-dimensional micro/nanostructures by integrating optical tweezers with chemical assembly. *Robotica*, 2005, **23**, 435–439.

ACKNOWLEDGEMENTS. We thank Prof. J. Yamanaka, Nagoya City University, Japan for sharing the photograph shown in Figure 6 and Drs C. S. Sundar and A. K. Arora for their support and encouragement.

Received 2 June 2011; revised accepted 17 October 2012